Cooperative Feedback for MIMO Interference Channels

Kaibin Huang
School of EEE, Yonsei University
Seoul, Korea
Email: huangkb@yonsei.ac.kr

Rui Zhang
Institute for Infocomm Research, A*STAR, Singapore
ECE Department, National University of Singapore
Email: rzhang@i2r.a-star.edu.sg

***Abstract*—Multi-antenna precoding effectively mitigates the interference in wireless networks. However, the precoding efficiency can be significantly degraded by the overhead due to the required feedback of channel state information (CSI). This paper addresses such an issue by proposing a systematic method of designing precoders for the two-user multiple-input-multiple-output (MIMO) interference channels based on finite-rate CSI feedback from receivers to their interferers, called *cooperative feedback*. Specifically, each precoder is decomposed into inner and outer precoders for nulling interference and improving the data link array gain, respectively. The inner precoders are further designed to suppress residual interference resulting from finite-rate cooperative feedback. To regulate residual interference due to precoder quantization, additional scalar cooperative feedback signals are designed to control transmitters' power using different criteria including applying interference margins, maximizing sum throughput, and minimizing outage probability. Simulation shows that such additional feedback effectively alleviates performance degradation due to quantized precoder feedback.**

I. INTRODUCTION

In multi-antenna wireless networks, precoding can effectively mitigate interference between coexisting links. This paper presents a new approach of efficiently implementing precoding in the two-user multiple-input-multiple-output (MIMO) interference channels by exchanging finite-rate channel state information (CSI). Specifically, precoders are designed to suppress interference to the interfered receivers based on their quantized CSI feedback, and the residual interference is regulated by additional feedback of power control signals.

Recently, progresses have been made in analyzing the capacity of multi-antenna interference channels. In particular, interference alignment techniques have been proposed for achieving the channel capacity for high signal-to-noise ratios (SNRs) [1]. Such techniques, however, have limited practicality due to their complexity, requirement of perfect global CSI and their sub-optimality for finite SNRs. This prompts the development of linear precoding algorithms for practical decentralized wireless networks [2]–[5]. For time-division multiplexing (TDD) multiple-input-single-output (MISO) interference channels, it is proposed in [2], [5] that forward-link beamformers can be adapted distributively based on reverse-link signal-to-interference-pluse-noise ratios (SINRs). Targeting the two-user MIMO interference channels, linear transceivers are designed in [3] under the constraint of one data stream per user and using different criteria including zero-forcing and minimum mean square error. In [4], the rate region for MISO interference channels is analyzed based on the cognitive radio principle, yielding a message passing algorithm for enabling distributive beamforming. The above prior work does not address the issue of finite-rate feedback though it is widely used in the practice to enable precoding. Neglecting feedback CSI errors in precoder designs leads to over optimistic network performance.

For MIMO precoding systems, the substantiality of CSI feedback overhead has motivated extensive research on CSI quantization algorithms, forming a field called *limited feedback* [6]. Recent limited feedback research has focused on MIMO downlink systems, where multiuser CSI feedback supports *space division multiple access* (SDMA) [7]. It has been found that the number of feedback bits per user has to increase with the transmit SNR so as to bound the throughput loss caused by feedback quantization [8]. Furthermore, such a loss can be reduced by exploiting *multiuser diversity* [9], [10]. Designing limited feedback algorithms for interference channels is more challenging due to the decentralized network architecture and the growth of feedback CSI. Cooperative feedback algorithms are proposed in [11] for a two-user cognitive radio network, where the secondary transmitter adjusts its beamformer to suppress interference to the primary receiver that cooperates by feedback to the secondary transmitter. This design is tailored for a MISO cognitive radio network and thus unsuitable for general MIMO interference channels, which motivates the current work.

We consider two coexisting MIMO links where all nodes employ equal numbers of antennas and linear precoding is enabled by quantized cooperative feedback. Channels are assumed to have i.i.d. Rayleigh fading. A systematic method is proposed for jointly designing linear precoders and equalizers under an orthogonality constraint, which decouples the links in the case of perfect feedback. To be specific, precoders and equalizers are decomposed into inner and outer components, where the former are designed to suppress residual interference caused by feedback errors and the latter to enhance link array gain. Second, additional scalar cooperative feedback, called *interference power control* (IPC) feedback, is proposed for controlling transmitters' power so as to regulate the residual interference. Specifically, the IPC feedback algorithms are designed using different criteria including fixed interference margin, maximum sum throughput, and minimum outage probability.

Notation: The superscript $\dagger$ represents matrix Hermitian transpose. The operator $[\mathbf{X}]_k$ gives the kth column of a matrix $\mathbf{X}$. Let $\preceq$, $\prec$, $\succeq$ and $\succ$ represent element-wise inequalities between two real vectors.

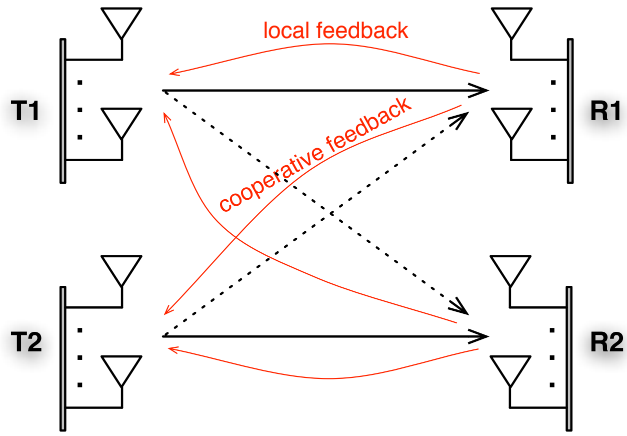

Fig. 1. MIMO interference channels with local and cooperative feedback.

II. SYSTEM MODEL

We consider two interfering wireless links as illustrated in Fig. 1, where the two pairs of transceivers are denoted as $(\mathsf{T}_1, \mathsf{R}_1)$ and $(\mathsf{T}_2, \mathsf{R}_2)$. Each transmitter/receiver has L antennas employed for suppressing the interference as well as supporting spatial multiplexing. These functions require CSI feedback from receivers to their interferers and intended transmitters, called *cooperative feedback* and *local feedback*, respectively. We assume perfect CSI estimation and local feedback, allowing the current design to focus on suppressing interference caused by cooperative feedback quantization. All channels are assumed to follow independent blocking fading. The channel coefficients are samples of i.i.d. $\mathcal{CN}(0,1)$ random variables. Let $\mathbf{H}_{mn}$ denote a $L \times L$ i.i.d. $\mathcal{CN}(0,1)$ matrix representing fading of the channel from T_n to R_m. Then the interference channels are modeled as $\{\nu \mathbf{H}_{mn}\}$ and the data channels as $\{\mathbf{H}_{mm}\}$ where $m, n \in \{1, 2\}$ and $m \neq n$. The factor $\nu < 1$ quantifies the difference in transmission distance between the data and interference links.

Each link supports $M \leq L$ spatial data streams by linear precoding and equalization. To regulate residual interference caused by precoder feedback errors, the total transmission power of each transmitter is constrained by cooperative IPC feedback. For simplicity, the scalar IPC feedback is assumed perfect since it requires much less overhead than the precoder feedback. Each transmitter uses identical transmission power for all spatial streams, represented by P_n for T_n with $n = 1, 2$ and the maximum $P_{\max}$. Assume that all additive white noise samples are i.i.d. $\mathcal{CN}(0,1)$ random variables. Let $\mathbf{G}_m$ and $\mathbf{F}_m$ denote the linear equalizer used by R_m and the linear precoder applied at T_m, respectively. Thus the receive signal-to-interference-plus-noise ratio (SINR) at R_m for the ℓth stream can be written as

$$\mathsf{SINR}_m^{[\ell]} := \frac{P_m |[\mathbf{G}_m]_\ell^\dagger \mathbf{H}_{mm} [\mathbf{F}_m]_\ell|^2}{1 + P_n \nu \|[\mathbf{G}_m]_\ell^\dagger \mathbf{H}_{mn} \mathbf{F}_n\|^2}, \quad m \neq n. \quad (1)$$

Two performance metrics, ergodic throughput and outage probability, are considered. The total ergodic throughput of both links, called *sum throughput*, is defined as

$$\bar{C} := \sum_{m=1}^{2} \sum_{\ell=1}^{M} \mathbb{E}\left[\log_2\left(1 + \mathsf{SINR}_m^{[\ell]}\right)\right] \quad (2)$$

where $\mathsf{SINR}_m^{[\ell]}$ is given in (1). Next, consider the scenario where the coding rates for all data streams are fixed at $\log_2(1+\theta)$ where θ is the receive SINR threshold for correct decoding. We define an outage event as one that the SINR of at least one data stream is smaller than θ. It follows that the outage probability is given by

$$P_{\mathsf{out}} := \Pr\left(\min_{m=1,2} \min_{1 \leq \ell \leq M} \mathsf{SINR}_m^{[\ell]} \leq \theta\right). \quad (3)$$

III. PRECODING WITH LIMITED FEEDBACK

A. Precoder Design

A pair of precoder and equalizer $(\mathbf{G}_m, \mathbf{F}_n)$ with $m \neq n$ are jointly designed under the following orthogonality constraint

$$\mathbf{G}_m^\dagger \mathbf{H}_{mn} \mathbf{F}_n = \mathbf{0}, \qquad m, n \in \{1, 2\}, m \neq n. \quad (4)$$

The constraint aims at decoupling the links and requires that $L \geq 2M$. A key step of the proposed design is to decompose the precoder $\mathbf{F}_n$ into an *inner precoder* $\mathbf{F}_n^{\mathsf{i}}$ and an *outer precoder* $\mathbf{F}_n^{\circ}$. Specifically, $\mathbf{F}_n = \mathbf{F}_n^{\mathsf{i}} \mathbf{F}_n^{\circ}$ where $\mathbf{F}_n^{\mathsf{i}}$ and $\mathbf{F}_n^{\circ}$ are $L \times M$ and $M \times M$ matrices, respectively, where the size of $\mathbf{F}_n^{\mathsf{i}}$ is minimized to reduce feedback overhead. Similarly, we decompose the equalizer $\mathbf{G}_m$ as $\mathbf{G}_m = \mathbf{G}_m^{\mathsf{i}} \mathbf{G}_m^{\circ}$ where $\mathbf{G}_m^{\mathsf{i}}$ is a $L \times N$ *inner equalizer* and $\mathbf{G}_m^{\circ}$ a $N \times M$ *outer equalizer*, where N is a design parameter under the constraints $N \geq M$ and $N \leq L - M$. The inner precoder/equalizer pair $(\mathbf{G}_m^{\mathsf{i}}, \mathbf{F}_n^{\mathsf{i}})$ is designed to enforce the constraint in (4) while the outer pair $(\mathbf{G}_m^{\circ}, \mathbf{F}_n^{\circ})$ enhances the link array gain as discussed in the sequel. It follows that

$$(\mathbf{G}_m^{\mathsf{i}})^\dagger \mathbf{H}_{mn} \mathbf{F}_n^{\mathsf{i}} = \mathbf{0}, \quad m \neq n. \quad (5)$$

Under this constraint, $(\mathbf{G}_m^{\mathsf{i}}, \mathbf{F}_n^{\mathsf{i}})$ are designed by decomposing $\mathbf{H}_{mn}$ using the singular value decomposition (SVD) as

$$\mathbf{H}_{mn} = \mathbf{V}_{mn} \begin{bmatrix} \sqrt{\lambda_{mn}^{[1]}} & & \mathbf{0} \\ & \ddots & \\ \mathbf{0} & & \sqrt{\lambda_{mn}^{[L]}} \end{bmatrix} \mathbf{U}_{mn}^\dagger, \quad m \neq n \quad (6)$$

where the unitary matrices $\mathbf{V}_{mn}$ and $\mathbf{U}_{mn}$ consist of the left and right singular vectors of $\mathbf{H}_{mn}$ as columns, respectively, and $\left\{\lambda_{mn}^{[\ell]}\right\}$ denote the eigenvalues of $\mathbf{H}_{mn}\mathbf{H}_{mn}^\dagger$ following the descending order. Let $\mathcal{A}$ and $\mathcal{B}$ be two subsets of the indices $\{1, 2, \cdots, L\}$ with $|\mathcal{A}| = N$, $|\mathcal{B}| = M$, and $\mathcal{A} \cap \mathcal{B} = \emptyset$. The constraint in (5) can be satisfied by choosing

$$\mathbf{G}_m^{\mathsf{i}} = \{[\mathbf{V}_{mn}]_k \mid k \in \mathcal{A}\} \text{ and } \mathbf{F}_n^{\mathsf{i}} = \{[\mathbf{U}_{mn}]_k \mid k \in \mathcal{B}\}. \quad (7)$$

Given $(\mathbf{G}_m^{\mathsf{i}}, \mathbf{F}_m^{\mathsf{i}})$, the outer pair $(\mathbf{G}_m^{\circ}, \mathbf{F}_m^{\circ})$ are jointly designed based on the SVD of the $N \times M$ effective channels

$\mathbf{H}^{\circ}_{mm} := \mathbf{G}^{\mathsf{i}}_m \mathbf{H}_{mm} \mathbf{F}^{\mathsf{i}}_m$:

$$\mathbf{H}^{\circ}_{mm} = \mathbf{V}_{mm} \begin{bmatrix} \sqrt{\lambda^{[1]}_{mm}} & & \mathbf{0} \\ & \ddots & \\ \mathbf{0} & & \sqrt{\lambda^{[M]}_{mm}} \\ \mathbf{0} & \cdots & \mathbf{0} \end{bmatrix} \mathbf{U}^{\dagger}_{mm}. \quad (8)$$

Note that the elements of $\mathbf{H}^{\circ}_{mm}$ are i.i.d. $\mathcal{CN}(0,1)$ random variables and their distributions are independent of $(\mathbf{G}^{\mathsf{i}}_m, \mathbf{F}^{\mathsf{i}}_m)$ since $\mathbf{H}_{mm}$ is isotropic. To transmit data through the eigenmodes of $\mathbf{H}_{mm}$, $\mathbf{G}^{\circ}_m$ and $\mathbf{F}^{\circ}_m$ are chosen as

$$\mathbf{G}^{\circ}_m = \{[\mathbf{V}_{mm}]_1, [\mathbf{V}_{mm}]_2, \cdots, [\mathbf{V}_{mm}]_M\} \text{ and } \mathbf{F}^{\circ}_m = \mathbf{U}_{mm}.$$

With perfect CSI feedback, the above precoder and equalizer joint design converts each data link into M parallel spatial channels which are free of interference.

Note that increasing N enhances the array gain of both links. Specifically, the expectations of the SNRs increase with N. Thus, N should take its maximum $(L-M)$. However, maximizing N need not be optimal for the link performance in the case of quantized feedback as discussed in the sequel.

B. Quantized Precoder Feedback

In this section, we choose the index sets $\mathcal{A}$ and $\mathcal{B}$ in (7) with the objective of suppressing the residual interference caused by precoder feedback errors.

Recall that the precoding at T_n is enabled by quantized cooperative feedback of $\mathbf{F}^{\mathsf{i}}_n$ from R_m with $m \neq n$. Let $\hat{\mathbf{F}}^{\mathsf{i}}_n$ denote the quantized version of $\mathbf{F}^{\mathsf{i}}_n$ and define the resultant quantization error ϵ_n as

$$\epsilon_n := 1 - \frac{\|(\mathbf{F}^{\mathsf{i}}_n)^{\dagger} \hat{\mathbf{F}}^{\mathsf{i}}_n\|^2_{\mathsf{F}}}{M}, \quad n = 1, 2 \quad (9)$$

where $0 \leq \epsilon_n \leq 1$. The error ϵ_n is zero in the case of perfect cooperative feedback, namely $\mathbf{F}^{\mathsf{i}}_n = \hat{\mathbf{F}}^{\mathsf{i}}_n$. A nonzero error results in violation of the orthogonality constraint in (5)

$$\mathbf{G}^{\mathsf{i}}_m \mathbf{H}_{mn} \hat{\mathbf{F}}^{\mathsf{i}}_n \neq 0, \quad m \neq n. \quad (10)$$

The resultant residual interference from T_n to the ℓth data stream of R_m has the power

$$I^{[\ell]}_{mn} := P_n \nu \|[\mathbf{G}^{\circ}_m]^{\dagger}_{\ell} (\mathbf{G}^{\mathsf{i}}_m)^{\dagger} \mathbf{H}_{mn} \hat{\mathbf{F}}^{\mathsf{i}}_n \mathbf{F}^{\circ}_n\|^2, \quad m \neq n. \quad (11)$$

Next, we choose $\mathcal{A}$ and $\mathcal{B}$ in (7) by minimizing an upper bound on the residual interference power as follows. Based on (7), (6) can be rewritten as

$$\mathbf{H}_{mn} = \begin{bmatrix} \mathbf{B}_m & \mathbf{G}^{\mathsf{i}}_m \end{bmatrix} \mathbf{\Sigma}_{mn} \begin{bmatrix} \mathbf{F}^{\mathsf{i}}_n & \mathbf{C}_n \end{bmatrix}^{\dagger} \quad (12)$$

where $\mathbf{\Sigma}_{mn} := \mathbf{\Pi} \ \mathrm{diag}\left(\sqrt{\lambda^{[1]}_{mn}}, \sqrt{\lambda^{[1]}_{mn}}, \cdots, \sqrt{\lambda^{[L]}_{mn}}\right) \mathbf{\Pi}^{\dagger}$ with $\mathbf{\Pi}$ being an arbitrary permutation matrix that rearranges the order of the singular values along the matrix diagonal. The columns of the matrices $\mathbf{B}_m$ and $\mathbf{C}_n$ comprise the $(L-N)$ left and $(L-M)$ right singular vectors of $\mathbf{H}_{mn}$, respectively, which are determined by $\mathbf{\Pi}$. Let the set $\mathcal{D}_{mn}$ contain the last N elements along the diagonal of $\mathbf{\Sigma}_{mn}$.

Lemma 1. *The interference power $I^{[\ell]}_{mn}$ in* (11) *can be upper bounded as*

$$I^{[\ell]}_{mn} \leq M \nu P_n \epsilon_n \max_{\alpha \in \mathcal{D}_{mn}} \alpha^2, \quad m \neq n. \quad (13)$$

Readers can refer to the full paper [12] for the proofs of the above lemma as well as analytical results in the sequel. Minimizing the upper bound in (13) gives that $\mathcal{D}_{mn}$ consists of the N smallest singular values of $\mathbf{H}_{mn}$. Equivalently, $\mathbf{\Pi}$ is an identity matrix and thus $\mathbf{G}^{\mathsf{i}}_m$ and $\mathbf{F}^{\mathsf{i}}_n$ are given as

$$\begin{aligned} \mathbf{G}^{\mathsf{i}}_m &= \{[\mathbf{V}_{mn}]_{L-N+1}, [\mathbf{V}_{mn}]_{L-N+1}, \cdots, [\mathbf{V}_{mn}]_L\} \\ \mathbf{F}^{\mathsf{i}}_n &= \{[\mathbf{U}_{mn}]_1, [\mathbf{U}_{mn}]_2, \cdots, [\mathbf{U}_{mn}]_M\}. \end{aligned} \quad (14)$$

Then (13) can be simplified as

$$I^{[\ell]}_{mn} \leq M \nu P_n \lambda^{[L-N+1]}_{mn} \epsilon_n, \quad \forall\ 1 \leq \ell \leq M, m \neq n. \quad (15)$$

Note that the above upper bound on $I^{[\ell]}_{mn}$ is independent of the stream index ℓ. On one hand, the upper bound reduces with decreasing N. On the other hand, as mentioned earlier, larger N increases link array gain. These opposite effects of N on link performance make it an important parameter for precoder optimization. Finding the optimal N is mathematically intractable but a numerical search is straightforward.

IV. Interference Power Control Feedback

A. Fixed Interference Margin

The receiver R_m sends the IPC signal, denoted as η_n, to the interferer T_n for controlling its transmission power as

$$P_n = \min(\eta_n, P_{\max}), \quad n = 1, 2. \quad (16)$$

The scalar η_n is designed to prevent the per-stream interference power at R_m from exceeding a fixed margin τ with $\tau > 0$, namely $I^{[\ell]}_{mn} \leq \tau$ for all $0 \leq \ell \leq M$. A sufficient condition for satisfying such constraints is to upper bound the right hand side of (15) by τ. It follows that

$$\eta_n := \frac{\tau}{M \nu \lambda^{[L-N+1]}_{mn} \epsilon_n}, \quad m \neq n. \quad (17)$$

Given τ, a lower bound A_{IM} on the sum throughput $\bar{C}$, called the *achievable throughput*, is obtained from (2) as

$$A_{\mathsf{IM}} = \sum_{m=1}^{2} \sum_{\ell=1}^{M} \log_2 \left(1 + \frac{\min(\eta_m, P_{\max}) \lambda^{[\ell]}_{mm}}{1 + \tau}\right) \quad (18)$$

where η_m is given (17).

It is infeasible to derive the optimal value of τ for either maximizing A_{IM} in (18) or minimizing P_{out} in (3). However, for $P_{\max}$ being either large or small, simple insight into choosing τ can be derived as follows. The residual interference power decreases continuously with reducing $P_{\max}$. Intuitively, τ should be kept small for small $P_{\max}$. For large $P_{\max}$, the choice of τ is less intuitive since large τ lifts the constraints on the transmission power but causes stronger interference and vice versa. We show below that large τ is preferred for large $P_{\max}$. Let $\acute{\lambda}_k$ denote the eigenvalue of the Wishart matrix $\mathbf{H}\mathbf{H}^{\dagger}$ with $\mathbf{H}$ being an i.i.d. $N \times M$ $\mathcal{CN}(0,1)$ matrix. Define $\check{\lambda}_k$ similarly but with $\mathbf{H}$ being a $L \times L$ matrix.

Lemma 2. *For large $P_{\max}$, the achievable throughput is*

$$A_{\mathsf{IM}} = 2\sum_{\ell=1}^{M}\mathbb{E}\left[\log_2\left(1+\frac{\tau\acute{\lambda}_\ell}{(1+\tau)M\nu\check{\lambda}_{L-N+1}\epsilon_1}\right)\right]+o(1)\,.$$

It can be observed from the above result that the first order term of A_{IM} attains its maximum for $\tau\to\infty$. However, this term is finite even for asymptotically large $P_{\max}$ and τ, which is the inherent effect of residual interference.

Lemma 3. *For large $P_{\max}$, the outage probability is upper bounded as*

$$P_{\mathsf{out}} \le 2\Pr\left(\frac{\tau}{1+\tau}\times\frac{\acute{\lambda}_\ell}{M\nu\check{\lambda}_{L-N+1}\epsilon_1}<\theta\right)+o(1).$$

Similar remarks on Lemma 2 apply to Lemma 3.

B. Sum Throughput Criterion

In this section, an iterative IPC algorithm is designed for increasing the sum throughput $\bar{C}$ in (2). Since $\bar{C}$ is a non-convex function of transmission power, directly maximizing $\bar{C}$ does not yield a simple IPC algorithm. Thus, we resort to maximizing a lower bound A_{ST} (achievable throughput) on $\bar{C}$ instead, obtained from (2) and (15) as $A_{\mathsf{ST}}=\mathbb{E}[A]$ with

$$\begin{aligned} A \;&:= \sum_{\ell=1}^{M}\left[\log_2\left(1+\frac{P_1\lambda_{11}^{[\ell]}}{1+P_2M\nu\lambda_{12}^{[L-N+1]}\epsilon_2}\right)+\right.\\ &\qquad\left.\log_2\left(1+\frac{P_2\lambda_{22}^{[\ell]}}{1+P_1M\nu\lambda_{21}^{[L-N+1]}\epsilon_1}\right)\right]. \end{aligned} \tag{19}$$

Thus, the optimal transmission power pair is given as

$$(P_1^\star,P_2^\star)=\max_{P_1,P_2\in[0,P_{\max}]}A(P_1,P_2). \tag{20}$$

The objective function A remains non-convex and its maximum has no known closed-form. However, inspired by the message passing algorithm in [4], a sub-optimal search for $(P_1^\star,P_2^\star)$ can be derived using the fact that

$$\frac{\partial A(P_1^\star,P_2^\star)}{\partial P_m}=0\ \forall\ m=1,2.$$

To this end, the slopes of A are obtained using (19) as

$$\frac{\partial A(P_1,P_2)}{\partial P_m}=\mu_m+\psi_m-\rho_m \tag{21}$$

where

$$\begin{aligned}
\mu_m &:= \log_2 e\sum\nolimits_{\ell=1}^{M}\frac{\lambda_{mm}^{[\ell]}}{1+M\nu\lambda_{mn}^{[L-N+1]}\epsilon_nP_n+\lambda_{mm}^{[\ell]}P_m}\\
\psi_m &:= \log_2 e\sum\nolimits_{\ell=1}^{M}\frac{M\nu\lambda_{nm}^{[L-N+1]}\epsilon_m}{1+M\nu\lambda_{nm}^{[L-N+1]}\epsilon_mP_m+\lambda_{nn}^{[\ell]}P_n}\\
\rho_m &:= \frac{\log_2 eM^2\nu\lambda_{nm}^{[L-N+1]}\epsilon_m}{1+M\nu\lambda_{nm}^{[L-N+1]}\epsilon_mP_m}.
\end{aligned}$$

Note that based on available CSI, μ_m has to be computed at R_m and (ψ_m,ρ_m) at R_n with $n\neq m$. Therefore, based on (21), an iterative IPC feedback algorithm can be designed to have the following procedure.

Algorithm 1:

1) The transmitters T_1 and T_2 arbitrarily select the initial values for P_1 and P_2, respectively.
2) The transmitters broadcast their choices of transmission power to the receivers.
3) Given (P_1,P_2), the receiver R_1 computes (μ_1,ψ_2,ρ_2) and sends μ_1 and $(\psi_2-\rho_2)$ to T_1 and T_2, respectively. Likewise, R_2 computes (μ_2,ψ_1,ρ_1) and feeds back μ_2 and $(\psi_1-\rho_1)$ to T_2 and T_1, respectively.
4) The transmitters T_1 and T_2 update P_1 and P_2, respectively, using (21) and the following equation
$$P_m(k+1)=\min\left\{\left[P_m(k)+\frac{\partial A(P_1,P_2)}{\partial P_m}\Delta\gamma\right]^+,P_{\max}\right\}$$
where k is the iteration index and $\Delta\gamma$ a step size.
5) Repeat Steps 2) $-$ 4) till the maximum number of iterations is performed or the changes on (P_1,P_2) are sufficiently small.

C. Outage Probability Criterion

As the problem of minimizing P_{out} in (3) by power control is analytically intractable, the IPC algorithm is designed by minimizing an upper bound on P_{out}. Using (15), the SINR in (1) is lower bounded by $\widetilde{\mathsf{SINR}}_m^{[\ell]}$ where

$$\widetilde{\mathsf{SINR}}_m^{[\ell]}:=\frac{P_m\lambda_{mm}^{[\ell]}}{1+P_nM\nu\lambda_{mn}^{[L-N+1]}\epsilon_n},\quad m\neq n. \tag{22}$$

Therefore,

$$P_{\mathsf{out}}\ \le\ \Pr\left(\min_{m=1,2}\widetilde{\mathsf{SINR}}_m^{[M]}<\theta\right). \tag{23}$$

Minimizing the above upper bound on P_{out} is similar in the mathematical structure to the classic problem of optimal power control for single-antenna interference channels [13]. The optimal transmission power for minimizing the right hand side of (23) solves the following optimization problem

$$\begin{aligned} &(P_1^\star,P_2^\star)=\arg\min_{P_1,P_2\in[0,P_{\max}]}(P_1,P_2)\\ &\text{s.t.}\ \min_{m=1,2}\widetilde{\mathsf{SINR}}_m^{[M]}(P_1,P_2)>\theta \end{aligned} \tag{24}$$

where the first minimization implies that $(P_1^\star,P_2^\star)\preceq(P_1,P_2)$ for all (P_1,P_2) that satisfies the constraint in (24) as well as $(0,0)\preceq(P_1,P_2)\preceq(P_{\max},P_{\max})$, called *feasible* power pairs. Using (22) and (24), the constraint in (24) can be written as

$$P_m\ge a_m+b_{mn}P_n,\quad m\neq n \tag{25}$$

where $a_m:=\frac{\theta}{\lambda_{mm}^{[M]}}$ and $b_{mn}:=\frac{M\nu\lambda_{mn}^{[L-N+1]}\epsilon_n\theta}{\lambda_{mm}^{[M]}}$. The minimum power $(\acute{P}_1,\acute{P}_2)$ that satisfies the constraints in (25) is

$$\acute{P}_m:=\frac{a_m+b_{mn}a_n}{1-b_{mn}b_{nm}},\quad m=1,2. \tag{26}$$

This expression gives optimal power control as stated below.

Proposition 1. *If $(P_1^\star,P_2^\star)$ in* (24) *exists, $(P_1^\star,P_2^\star)=(\acute{P}_1,\acute{P}_2)$ with $(\acute{P}_1,\acute{P}_2)$ given in* (26).

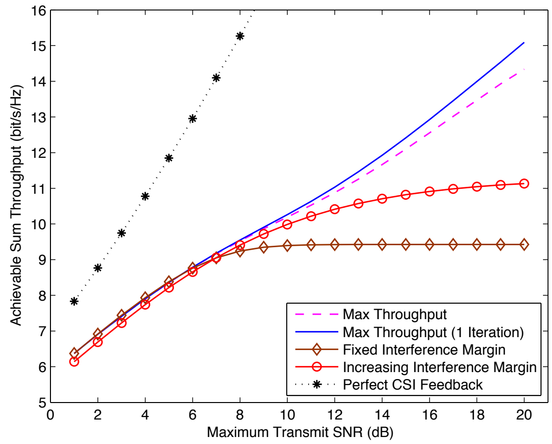

Fig. 2. Comparison of achievable sum throughput between different IPC feedback algorithms for the coupling factor $\nu = 0.2$.

Based on Proposition 1, the corresponding IPC feedback procedure is obtained as follows.

Algorithm 2:

1) The receiver R_1 computes b_{12} and transmits b_{12} to T_2. Similarly, R_2 computes b_{21} and feeds back b_{21} to T_1.
2) The receiver R_1 computes a_1 and communicates a_1 to T_1. Likewise, R_2 computes a_2 and feeds back a_2 to T_2.
3) The transmitters T_1 and T_2 compute $\acute{P}_1$ and $\acute{P}_2$, respectively and set their transmission power equal to $(\acute{P}_1, \acute{P}_2)$ if they are feasible. Otherwise, arbitrary transmission power is used.

V. Simulation Results

In the simulation, codebooks for quantizing $\mathbf{F}_1^{\mathsf{i}}$ and $\mathbf{F}_2^{\mathsf{i}}$ are randomly generated and have equal sizes. The simulation parameters are set as $L = 6$, $M = 2$, $N = 3$, and $B = 6$. The interference margin is either fixed at $\tau = 2$ or increased as $\tau = 0.4P_{\max}$.

Fig. 2 compares the achievable throughput of different IPC feedback algorithms. Significant coupling ($\nu = 0.2$) between links is observed to decrease achievable throughput dramatically with respect to perfect CSI feedback. For large $P_{\max}$, the IPC feedback Algorithm 1 designed for maximizing the achievable throughput is observed to provide substantial throughput gain over those based on interference margins. Furthermore, increasing τ with growing $P_{\max}$ gives higher throughput than fixed τ, which is consistent with Lemma 2.

Fig. 3 compares the outage probabilities and average transmit SNRs of different IPC feedback algorithms. With respect to the IPC feedback using increasing τ or with perfect feedback, Algorithm 2 dramatically decreases average transmission power. Moreover, Algorithm 2 yields lower outage probability than the two algorithms using τ. Finally, fixing τ causes P_{out} to saturate as $P_{\max}$ increases.

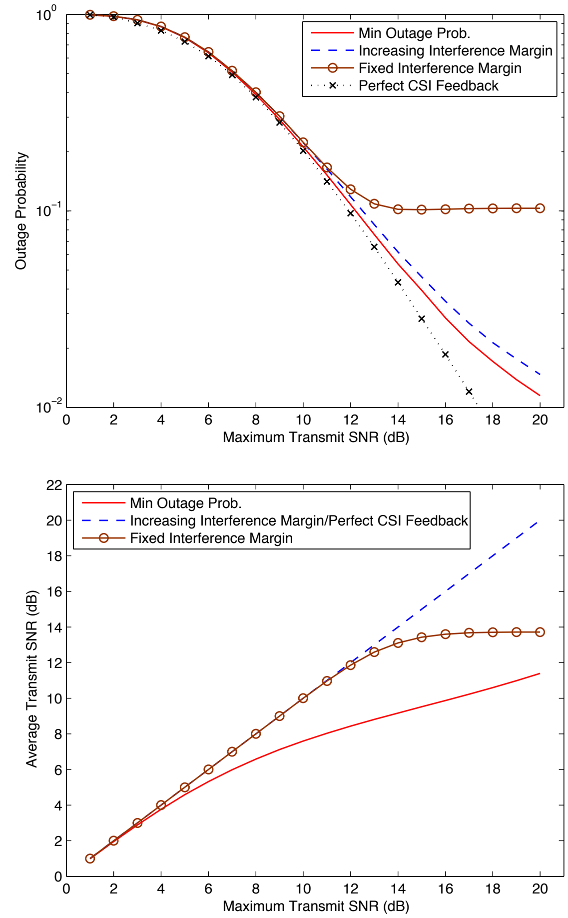

Fig. 3. Comparison of outage probability (upper) and average transmit SNR (lower) between different IPC feedback algorithms for the coupling factor $\nu = 0.05$.

References

[1] V. R. Cadambe and S. A. Jafar, "Interference alignment and the degrees of freedom for the k user interference channel," *IEEE Trans. on Inform. Theory*, vol. 54, pp. 3425–3441, Aug. 2008.

[2] R. Zakhour and D. Gesbert, "Distributed multicell-MISO precoding using the layered virtual SINR framework," *to appear in IEEE Trans. Wireless Comm.*

[3] C. B. Chae, I. Hwang, R. W. H. Jr., and V. Tarokh, "Interference aware-coordinated beamforming system in a two-cell environment," *submitted to IEEE Journal on Selected Areas in Communications*.

[4] R. Zhang and S. Cui, "Cooperative interference management with MISO beamforming," *to appear in IEEE Trans. on Sig. Proc.*

[5] H. Dahrouj and W. Yu, "Coordinated beamforming for the multicell multi-antenna wireless system," *IEEE Trans. on Wireless Communications*, vol. 9, pp. 1748–1759, May 2010.

[6] D. J. Love, R. W. Heath, V. K. N. Lau, D. Gesbert, B. D. Rao, and M. Andrews, "An overview of limited feedback in wireless communication systems," *IEEE Journal on Sel. Areas in Communications*, vol. 26, no. 8, pp. 1341–1365, 2008.

[7] D. Gesbert, M. Kountouris, R. W. Heath Jr., C.-B. Chae, and T. Salzer, "From single user to multiuser communications: Shifting the MIMO paradigm," *IEEE Signal Processing Magazine*, vol. 24, no. 5, pp. 36–46, 2007.

[8] N. Jindal, "MIMO broadcast channels with finite-rate feedback," *IEEE Trans. on Inform. Theory*, vol. 52, pp. 5045–5060, Nov. 2006.

[9] M. Sharif and B. Hassibi, "On the capacity of MIMO broadcast channels with partial side information," *IEEE Trans. on Inform. Theory*, vol. 51, pp. 506–522, Feb. 2005.

[10] K.-B. Huang, J. G. Andrews, and R. W. Heath Jr., "Performance of orthogonal beamforming for SDMA systems with limited feedback," *IEEE Trans. on Veh. Technology*, vol. 58, pp. 152–164, Jan. 2009.

[11] K. Huang and R. Zhang, "Cooperative feedback for multi-antenna cognitive radio networks," *to appear in IEEE Trans. on Sig. Proc.*

[12] K. Huang and R. Zhang, "Cooperation in MIMO interference channels by limited feedback," *Preprint: http://ee.yonsei.ac.kr/huangkb/*.

[13] G. Foschini and Z. Miljanic, "A simple distributed autonomous power control algorithm and its convergence," *IEEE Trans. on Veh. Technology*, vol. 42, pp. 641–646, Apr. 1993.